



# Transient, Steady-State and Total Dynamic Responses of Mindlin Viscoelastic Plates Subjected to Harmonic Transversal Load and In-Plane Compression

Nasrin Jafari<sup>1</sup>

Received: 13 June 2022 / Revised: 13 July 2022 / Accepted: 14 July 2022 / Published online: 8 August 2022  
© Krishtel eMaging Solutions Private Limited 2022

## Abstract

**Purpose** This research proves a novel closed-form solution for the forced vibration analysis of a Mindlin viscoelastic plate subjected to harmonic transversal load and constant in-plane compression, simultaneously.

**Method** The excitation frequency of the harmonic transversal load is considered as equal to the natural frequency of the viscoelastic plate. The viscoelastic properties obey the Boltzmann integral law with constant bulk modulus. The displacement field is approximated by the product of a known geometrical function and an unknown time function. The simple hp cloud method is employed for discretization. Calculating the natural and viscous damping frequencies, geometry, mass and stiffness matrices in the Laplace–Carson domain, and introducing the best values to replace the Laplace parameter, the dynamic responses of Mindlin viscoelastic plates are determined.

**Results and Conclusion** The transient, steady-state and total dynamic responses of moderately thick viscoelastic plates are explicitly formulated in the time domain based on the elastic bending analysis at time zero, for the first time. In the numerical results, the effects of material properties and loading on the total dynamic responses are investigated.

**Keywords** Dynamic response · Forced vibration analysis · Moderately thick viscoelastic plates · Steady-state response · Transient response

## Introduction

As the use of time-dependent composite materials increases in industries, the use of viscoelastic theories has been increasing recently. Due to the damping property of viscoelastic materials, the dynamic analysis of viscoelastic plates subjected to harmonic load is one of the most interesting problems in the structural vibration field. Vibration control is needed to control noise in engineering systems and to reduce vibration levels. Wang and Tsai [1] employed the finite element method to analyze the quasi-static and dynamic responses of linear viscoelastic plates with constant Poisson's ratio. Ilyasov and Akoz [2] considered the static and dynamic behavior of simply supported viscoelastic triangular plates subjected to static and dynamic loads

employing the Boltzmann–Volterra principle. Eshmatov [3] studied the geometrically nonlinear vibration and dynamic stability analysis of viscoelastic orthotropic rectangular plates based on the Kirchhoff–Love hypothesis and Reissner–Mindlin generalized theory. Abdoun et al. [4] investigated the asymptotic numerical method for the forced harmonic vibration analysis of viscoelastic structures. Gupta et al. [5] presented the vibration analysis of clamped viscoelastic rectangular plates with varying thickness, linearly in one and parabolically in other direction. Li and Cheng [6] studied the dynamic behavior of viscoelastic plates by considering higher-order shear effects and finite deformations. Shariyat [7] investigated the free vibration and dynamic buckling analyses of viscoelastic composite sandwich plates subjected to thermomechanical loads based on the double-superposition global–local theory. Mahmoudkhani et al. [8] considered the free and forced vibration analysis of sandwich plates with thick viscoelastic cores under wide-band random excitation. Temel and Sahan [9] studied the transient behavior of orthotropic viscoelastic thick plates under dynamic loads using the Laplace transformation. Amabili

✉ Nasrin Jafari  
jafarin@iut.ac.ir

<sup>1</sup> Department of Civil Engineering, Isfahan University of Technology, Isfahan 84156-83111, Iran

[10] investigated the nonlinear vibration analysis of viscoelastic rectangular plates using the Von Karman assumptions and Kelvin–Voigt solids. Wan and Zheng [11] considered the vibration and damping analysis of the five-layered constrained damping plates based on the theory of Donnell using the complex constant model. Khadem Moshir et al. [12] studied the free vibration analysis of moderately thick annular viscoelastic plates based on the perturbation technique. Amabili [13] presented the nonlinear vibration analysis of viscoelastic rectangular plates derivation from viscoelasticity and experimental validation. Balasubramanian et al. [14] studied the geometrically nonlinear vibration analysis of rubber viscoelastic rectangular plates with fixed edges and identified the increase of damping with the vibration amplitude, experimentally and numerically. Zhou and Wang [15] studied the transverse vibration and dynamic stability of the axially moving viscoelastic plates based on the Kelvin–Voigt model. Rouzegar and Davoudi [16] investigated the forced vibration analysis of smart laminated viscoelastic composite plates integrated with a piezoelectric layer using the RPT finite element approach. Silva et al. [17] presented the uncertainty propagation and numerical evaluation for the nonlinear dynamic analysis of viscoelastic sandwich plates by performing the Karhunen–Loeve expansion technique. Sofiyev et al. [18] considered the free vibration and dynamic stability analyses of functionally graded viscoelastic plates subjected to compressive load and resting on elastic foundations. Ojha and Dwivedy [19] studied the dynamic analysis of a three-layered sandwich plate with thin composite layers and LPRE-based viscoelastic core. Amabili et al. [20] considered the nonlinear vibrations and nonlinear damping of fractional viscoelastic rectangular plates using a fractional linear solid model, experimentally and numerically. Zamani [21] investigated the free vibration analysis of viscoelastic plates employing single-term Bubnov–Galerkin, least squares, and point collocation methods. Jafari and Azhari [22] presented the free vibration analysis of moderately thick viscoelastic plates based on the free vibration analysis of elastic plates. Jafari [23] investigated the non-harmonic resonance of Mindlin viscoelastic plates subjected to time-dependent decreasing exponential transversal distributed loads. Jafari and Azhari [24] studied the dynamic stability analysis of moderately thick viscoelastic plates subjected to constant and harmonic in-plane compression based on the free vibration analysis of elastic plates.

Due to the difficulty and complexity of the equations, there are few articles on the forced vibration analysis of moderately thick viscoelastic plates. Also, there are not any closed-form solutions for the total dynamic responses of Mindlin viscoelastic plates subjected to harmonic transversal load and in-plane compression, simultaneously. The present paper investigates the forced vibration analysis of moderately thick viscoelastic plates under

harmonic transversal and constant in-plane compressive loads, simultaneously. The excitation frequency of the harmonic load is investigated as equal to the natural frequency. The stress–strain relation is written based on the Boltzmann superposition principle with constant bulk modulus for linear viscoelastic materials. The displacement field is approximated using the separation of variables technique by the product of a known geometrical function and an unknown time function. The Laplace transform is employed to convert equations from the time domain to the Laplace domain. The simple hp cloud method is employed for discretization. Calculating the natural and viscous damping frequencies, geometry and mass matrices, stiffness matrix in the Laplace–Carson domain, and finding the best values to replace the Laplace parameter, the unknown coefficients of the time function are determined. Finally, a closed-form solution is extracted while the transient, steady-state and total dynamic responses of Mindlin viscoelastic plates under out-of-plane and in-plane loadings are explicitly formulated in the time domain for the first time.

This paper is organized as follows: The extraction of equations of forced vibration analysis of moderately thick viscoelastic plates is described in Sect. 2. The numerical results are presented in Sect. 3. Section 4 presents the conclusions. The extraction of equations of forced vibration analysis of Bernoulli viscoelastic beams is described in Appendix 1.

## Governing Equations

### Kinematic Relations

The time-dependent displacement field is defined using the first-order shear deformation theory as:

$$\begin{cases} u(x,y,z,t) \\ v(x,y,z,t) \\ w(x,y,z,t) \end{cases} = \begin{cases} u_0(x,y,t) - z\theta_x(x,y,t) \\ v_0(x,y,t) - z\theta_y(x,y,t) \\ w(x,y,t) \end{cases}, \quad (1)$$

in which  $\theta_x$  and  $\theta_y$  denote the rotations around  $y$  and  $x$  axes, respectively.  $u_0$  and  $v_0$  are the in-plane displacements and  $w(x,y,t)$  is an out-of-plane displacement of the middle surface.

According to the small deformation theory, the in-plane and out-of-plane solutions of a plate are uncoupled [25]. So, assuming the in-plane compressions to be less than the critical buckling load, the in-plane displacements of the middle surface can be removed for out-of-plane analysis.

Omitting the in-plane displacements, the strain–displacement relations can be given as follows:

$$\boldsymbol{\epsilon}(x,y,z,t) = \begin{Bmatrix} -z\theta_{x,x} \\ -z\theta_{y,y} \\ -z(\theta_{x,y} + \theta_{y,x}) \\ w_{,x} - \theta_x \\ w_{,y} - \theta_y \end{Bmatrix}. \tag{2}$$

### Constitutive Equations

According to the Boltzmann superposition principle, the stress–strain relations of a linear viscoelasticity can be written as [26]:

$$\boldsymbol{\sigma}(x,y,z,t) = \mathbf{C}(t)\boldsymbol{\epsilon}(x,y,z,0) + \int_0^t \mathbf{C}(t - \tau)\dot{\boldsymbol{\epsilon}}(x,y,z,\tau)d\tau, \tag{3}$$

where  $\mathbf{C}(t)$  is the time-dependent relaxed modulus tensor,  $\dot{\boldsymbol{\epsilon}}(t) = \partial\boldsymbol{\epsilon}/\partial t$ , and the stress vector  $\boldsymbol{\sigma}(x,y,z,t)$  is defined as:

$$\boldsymbol{\sigma}(x,y,z,t) = \langle \sigma_x \ \sigma_y \ \tau_{xy} \ \tau_{xz} \ \tau_{yz} \rangle^T. \tag{4}$$

For isotropic materials, Eqs. (5–6) are always valid:

$$K(t) = \frac{E(t)}{3(1 - 2\nu(t))}, \tag{5}$$

$$G(t) = \frac{E(t)}{2(1 + \nu(t))}, \tag{6}$$

where  $K(t)$ ,  $G(t)$  and  $E(t)$  are the bulk, shear, and elastic moduli and  $\nu(t)$  is the Poisson ratio.

Assuming the constant bulk modulus:

$$K(t) = K. \tag{7}$$

Substituting Eqs. (5) and (7) into Eq. (6), Eq. (8) is obtained:

$$G(t) = \frac{3K}{2} \frac{(1 - 2\nu(t))}{(1 + \nu(t))} = G_0\eta(t), G_0 = \frac{3K}{2}, \eta(t) = \frac{(1 - 2\nu(t))}{(1 + \nu(t))}, \tag{8}$$

where the dimensionless relaxation function of a viscoelastic

$$\mathbf{u}(x,y,t) = \begin{Bmatrix} w(x,y,t) \\ \theta_x(x,y,t) \\ \theta_y(x,y,t) \end{Bmatrix} = \begin{Bmatrix} w(x,y, t = 0) \\ \theta_x(x,y, t = 0) \\ \theta_y(x,y, t = 0) \end{Bmatrix} F(t) = \mathbf{u}^0 F(t), \mathbf{u}^0 = \mathbf{u}(x,y, t = 0). \tag{17}$$

material can be defined by three coefficients as follows [22, 24, 27]:

$$\eta(t) = c_1 + c_2 \exp(-\lambda t), \lambda = 1/t_s. \tag{9}$$

$c_1$  and  $c_2$  are constant parameters and  $t_s$  is the relaxation time of a viscoelastic material.

Substituting Eqs. (7–9) into Eqs. (5–6), the time-dependent elastic modulus and the time-dependent Poisson ratio can be given as:

$$E(t) = \frac{9K\eta(t)}{2 + \eta(t)}, \tag{10}$$

$$\nu(t) = \frac{1 - \eta(t)}{2 + \eta(t)}. \tag{11}$$

### Equation of Motion

The equilibrium equation of a moderately thick viscoelastic plate subjected to harmonic transversal loading  $q(t)$ , and in-plane compressive forces  $N_x$  and  $N_y$ , as illustrated in Fig. 1, can be stated as:

$$\delta U - \delta V_1 - \delta V_2 - \delta T = 0. \tag{12}$$

The variations of the strain,  $\delta U$ , potentials,  $\delta V_1$  and  $\delta V_2$ , and kinetic,  $\delta T$ , energies are written as:

$$\delta U = \int_V \left( \boldsymbol{\epsilon}(0)^T \mathbf{C}(t) + \int_0^t \dot{\boldsymbol{\epsilon}}(\tau)^T \mathbf{C}(t - \tau) d\tau \right) \delta \boldsymbol{\epsilon} dV, \tag{13}$$

$$\delta V_1 = \int_A \left[ N_x \frac{\partial w}{\partial x} \frac{\partial \delta w}{\partial x} + N_y \frac{\partial w}{\partial y} \frac{\partial \delta w}{\partial y} \right] dA, \tag{14}$$

$$\delta V_2 = \int_A q(t) \delta w dA, \tag{15}$$

$$\delta T = - \int_V \rho \left[ \frac{\partial^2 u}{\partial t^2} \delta u + \frac{\partial^2 v}{\partial t^2} \delta v + \frac{\partial^2 w}{\partial t^2} \delta w \right] dV, \tag{16}$$

where  $\rho$  is the plate density.

### Separation of Variables

The displacement vector can be approximated using the separation of variables method as follows:

The variation and the rate of displacement vector can be given as:

$$\delta \mathbf{u}(x,y,t) = \mathbf{u}^0 \delta F, \tag{18}$$

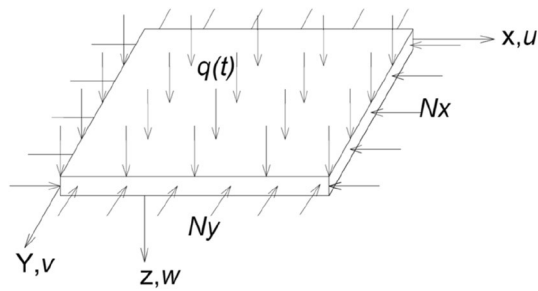


**Fig. 1** A viscoelastic plate subjected to harmonic transversal load and in-plane compressions

$$\dot{\mathbf{u}}(x,y,t) = \mathbf{u}^0 \dot{F}(t). \tag{19}$$

Using Eqs. (17–19), the strain vector, the variation of strain vector, the rate of strain vector, and the variation of out-of-plane displacement are obtained as:

$$\boldsymbol{\varepsilon}(x,y,z,t) = \boldsymbol{\varepsilon}(x,y,z,t=0)F(t) = \boldsymbol{\varepsilon}^0 F(t), \tag{20}$$

$$\delta \boldsymbol{\varepsilon} = \boldsymbol{\varepsilon}^0 \delta F, \tag{21}$$

$$\dot{\boldsymbol{\varepsilon}} = \boldsymbol{\varepsilon}^0 \dot{F}(t), \tag{22}$$

$$\delta w = w^0 \delta F. \tag{23}$$

**Discretization**

There are several numerical methods for discretizing equations in the space domain. In this study, the simple hp cloud method is utilized, [27].

The displacement vector can be discretized as:

$$\mathbf{u}^0 = \mathbf{N}\mathbf{U}^0, \mathbf{U}^0 = [\mathbf{U}_1^T \ \mathbf{U}_2^T \ \dots \ \mathbf{U}_N^T], \tag{24}$$

in which:

$$\mathbf{U}_i = \langle w_i \ \theta_{x_i} \ \theta_{y_i} \rangle^T \tag{25}$$

$$\delta U = \int_A \mathbf{U}^{0T} \mathbf{B}^T F(0) \mathbf{D}(t) \mathbf{B} \mathbf{U}^0 dA \delta F + \int_A \int_0^t \mathbf{U}^{0T} \mathbf{B}^T \dot{F}(\tau) \mathbf{D}(t-\tau) d\tau \mathbf{B} \mathbf{U}^0 dA \delta F, \tag{31}$$

and  $\mathbf{N}$  is the vector of basis functions. More details exist in Appendix 2.

Substituting Eqs. (17–25) into Eqs. (13–16), Eqs. (26–29) are derived:

$$\delta U = \int_V \mathbf{U}^{0T} \mathbf{B}^T F(0) \mathbf{C}(t) \mathbf{B} \mathbf{U}^0 \delta F dV + \int_V \int_0^t \mathbf{U}^{0T} \mathbf{B}^T \dot{F}(\tau) \mathbf{C}(t-\tau) d\tau \mathbf{B} \mathbf{U}^0 \delta F dV, \tag{26}$$

$$\delta V_1 = \int_A \mathbf{U}^{0T} \mathbf{B}_G^T F(t) \mathbf{N}_p \mathbf{B}_G \mathbf{U}^0 \delta F dA, \tag{27}$$

$$\delta V_2 = \int_A q(t) \mathbf{N}_w \mathbf{U}^0 \delta F dA, \tag{28}$$

$$\delta T = - \int_V \mathbf{U}^{0T} \mathbf{N}^T \mathbf{C}_m \ddot{F}(t) \mathbf{N} \mathbf{U}^0 \delta F dV. \tag{29}$$

The strain–displacement transformation matrices  $\mathbf{B}$  and  $\mathbf{B}_G$  are introduced in Sect. 2.9 and the matrix of in-plane compressive forces  $\mathbf{N}_p$  is defined as follows:

$$\mathbf{N}_p = \begin{bmatrix} N_x & 0 \\ 0 & N_y \end{bmatrix} = \alpha_1 N_{cr} \begin{bmatrix} 1 & 0 \\ 0 & k_1 \end{bmatrix}, k_1 = N_y/N_x, 0 \leq \alpha_1 < 1. \tag{30}$$

$N_{cr}$  is the critical compressive load of a viscoelastic plate at time zero and  $\alpha_1$  is an arbitrary constant coefficient.

**Harmonic Transversal Load**

For Mindlin viscoelastic plates,  $\Omega$  is defined as the fundamental natural frequency calculated by the free vibration analysis of moderately thick viscoelastic plates at time zero [22]. If the plate is subjected to in-plane compression too, the natural frequency  $\omega_0$  is decreased  $\omega_0 \cong \Omega \sqrt{1 - \alpha_1}, 0 \leq \alpha_1 < 1$ , [24]. In this paper, the plate is subjected to harmonic transversal load  $q(t) = q \sin \omega_0 t$  and in-plane compressions, simultaneously. In other word, the excitation frequency is considered as equal to the natural frequency and the time-dependent behavior of the viscoelastic plate is studied.

**Integrating over the Thickness**

By integrating over the thickness of the plate, Eq. (26) can be rewritten as:

in which the time-dependent effective modulus tensor can be stated as:

$$\mathbf{D}(t) = \begin{bmatrix} \frac{E(t)h^3}{12(1-\nu(t)^2)} \begin{bmatrix} 1 & \nu(t) & 0 \\ \nu(t) & 1 & 0 \\ 0 & 0 & \frac{1-\nu(t)}{2} \end{bmatrix} & 0 \\ 0 & \frac{E(t)hk}{2(1+\nu(t))} \begin{bmatrix} 1 & 0 \\ 0 & 1 \end{bmatrix} \end{bmatrix}, \quad (32)$$

$h$  is the plate thickness and  $k$  is the shear correction factor of the first-order shear deformation theory.

Also, by integrating over the thickness of the plate, Eq. (29) can be stated as:

$$\delta T = - \int_A \mathbf{U}^{0T} \mathbf{N}^T \ddot{F}(t) \mathbf{D}_m \mathbf{N} \mathbf{U}^0 dA \delta F, \quad (33)$$

where the mass density matrix,  $\mathbf{D}_m$ , can be expressed as:

$$\mathbf{D}_m = \rho \begin{bmatrix} h & 0 & 0 \\ 0 & \frac{h^3}{12} & 0 \\ 0 & 0 & \frac{h^3}{12} \end{bmatrix}. \quad (34)$$

Substituting Eqs. (27–28, 31, 33) into Eq. (12), Eq. (35) is derived:

$$\begin{aligned} & \left\{ \int_A \mathbf{U}^{0T} \mathbf{B}^T \left( F(0) \mathbf{D}(t) + \int_0^t \dot{F}(\tau) \mathbf{D}(t-\tau) d\tau \right) \mathbf{B} \mathbf{U}^0 dA \right. \\ & - \alpha_1 N_{cr} \int_A \mathbf{U}^{0T} \mathbf{B}_G^T F(t) \begin{bmatrix} 1 & 0 \\ 0 & k_1 \end{bmatrix} \mathbf{B}_G \mathbf{U}^0 dA \\ & \left. + \int_A \mathbf{U}^{0T} \mathbf{N}^T \ddot{F}(t) \mathbf{D}_m \mathbf{N} \mathbf{U}^0 dA \right\} \delta F = \sin \omega_0 t \int_A q \mathbf{N}_w \mathbf{U}^0 dA \delta F \end{aligned} \quad (35)$$

Removing  $\delta F$  from Eq. (35), Eq. (36) is derived:

$$\begin{aligned} & \mathbf{U}^{0T} \left\{ \int_A \mathbf{B}^T \left( F(0) \mathbf{D}(t) + \int_0^t \dot{F}(\tau) \mathbf{D}(t-\tau) d\tau \right) \mathbf{B} dA \right\} \mathbf{U}^0 \\ & - \alpha_1 N_{cr} F(t) \mathbf{U}^{0T} \left( \int_A \mathbf{B}_G^T \begin{bmatrix} 1 & 0 \\ 0 & k_1 \end{bmatrix} \mathbf{B}_G dA \right) \mathbf{U}^0 \\ & + \ddot{F}(t) \mathbf{U}^{0T} \left( \int_A \mathbf{N}^T \mathbf{D}_m \mathbf{N} dA \right) \mathbf{U}^0 = \sin \omega_0 t \left( \int_A q \mathbf{N}_w dA \right) \mathbf{U}^0. \end{aligned} \quad (36)$$

### Transforming to Laplace Domain

Utilizing the Laplace transform, the convolution integral of Eq. (36) can be simplified as follows:

$$\begin{aligned} & \mathbf{U}^{0T} \left( \int_A \mathbf{B}^T F^* s \mathbf{D}^* \mathbf{B} dA \right) \mathbf{U}^0 - \alpha_1 N_{cr} F^* \mathbf{U}^{0T} \\ & \left( \int_A \mathbf{B}_G^T \begin{bmatrix} 1 & 0 \\ 0 & k_1 \end{bmatrix} \mathbf{B}_G dA \right) \mathbf{U}^0 + \ddot{F}^* \mathbf{U}^{0T} \left( \int_A \mathbf{N}^T \mathbf{D}_m \mathbf{N} dA \right) \mathbf{U}^0 \\ & = (\sin \omega_0 t)^* \left( \int_A q \mathbf{N}_w dA \right) \mathbf{U}^0, \end{aligned} \quad (37)$$

in which  $F^*$ ,  $\mathbf{D}^*$ ,  $\ddot{F}^*$  and  $(\sin \omega_0 t)^*$  are the Laplace transformation of  $F(t)$ ,  $\mathbf{D}(t)$ ,  $\ddot{F}(t)$  and  $\sin \omega_0 t$ , respectively.

### Steady-State Response

The time function is approximated as follows:

$$F(t) = A \sin \omega_0 t + B \cos \omega_0 t. \quad (38)$$

Hence, Eqs. (39–40) are derived:

$$\ddot{F}(t) = -A \omega_0^2 \sin \omega_0 t - B \omega_0^2 \cos \omega_0 t = -\omega_0^2 F(t), \quad (39)$$

$$\ddot{F}^* = -\omega_0^2 F^*. \quad (40)$$

Inserting Eq. (40) into Eq. (37), Eq. (41) is obtained:

$$\begin{aligned} & F^* \left\{ \mathbf{U}^{0T} \left( \int_A \mathbf{B}^T \overline{\mathbf{D}} \mathbf{B} dA \right) \mathbf{U}^0 - \alpha_1 N_{cr} \mathbf{U}^{0T} \left( \int_A \mathbf{B}_G^T \begin{bmatrix} 1 & 0 \\ 0 & k_1 \end{bmatrix} \mathbf{B}_G dA \right) \right. \\ & \left. \mathbf{U}^0 - \omega_0^2 \mathbf{U}^{0T} \left( \int_A \mathbf{N}^T \mathbf{D}_m \mathbf{N} dA \right) \mathbf{U}^0 \right\} \\ & = (\sin \omega_0 t)^* \left( \int_A q \mathbf{N}_w dA \right) \mathbf{U}^0, \overline{\mathbf{D}} = s \mathbf{D}^*. \end{aligned} \quad (41)$$

On the other hand:

$$F^* = \frac{A \omega_0 + B s}{s^2 + \omega_0^2}, (\sin \omega_0 t)^* = \frac{\omega_0}{s^2 + \omega_0^2}. \quad (42)$$

Substituting Eqs. (42) into Eq. (41), Eq. (43) is derived:

$$\begin{aligned} & \frac{A \omega_0 + B s}{s^2 + \omega_0^2} \left\{ \mathbf{U}^{0T} \left( \int_A \mathbf{B}^T \overline{\mathbf{D}} \mathbf{B} dA \right) \mathbf{U}^0 - \alpha_1 N_{cr} \mathbf{U}^{0T} \right. \\ & \left. \left( \int_A \mathbf{B}_G^T \begin{bmatrix} 1 & 0 \\ 0 & k_1 \end{bmatrix} \mathbf{B}_G dA \right) \mathbf{U}^0 - \omega_0^2 \mathbf{U}^{0T} \left( \int_A \mathbf{N}^T \mathbf{D}_m \mathbf{N} dA \right) \mathbf{U}^0 \right\} \\ & = \frac{\omega_0}{s^2 + \omega_0^2} \int_A q \mathbf{N}_w dA \mathbf{U}^0. \end{aligned} \quad (43)$$

Equation (43) can be rewritten as follows:

$$\begin{aligned} & (A \omega_0 + B s) \left\{ \mathbf{U}^{0T} \left( \int_A \mathbf{B}^T \overline{\mathbf{D}} \mathbf{B} dA \right) \mathbf{U}^0 - \alpha_1 N_{cr} \mathbf{U}^{0T} \right. \\ & \left. \left( \int_A \mathbf{B}_G^T \begin{bmatrix} 1 & 0 \\ 0 & k_1 \end{bmatrix} \mathbf{B}_G dA \right) \mathbf{U}^0 - \omega_0^2 \mathbf{U}^{0T} \left( \int_A \mathbf{N}^T \mathbf{D}_m \mathbf{N} dA \right) \mathbf{U}^0 \right\} \\ & = \omega_0 \left( \int_A q \mathbf{N}_w dA \right) \mathbf{U}^0. \end{aligned} \quad (44)$$

Defining the stiffness matrix in the Laplace–Carson domain  $\overline{\mathbf{K}}$ , geometry matrix  $\mathbf{K}_G$ , mass matrix  $\mathbf{K}_m$ , and load vector  $\mathbf{R}$  as follows:

$$\bar{\mathbf{K}} = \int_A \mathbf{B}^T \bar{\mathbf{D}} \mathbf{B} dA = \left( \int_A \mathbf{B}_b^T \bar{\mathbf{D}}_b \mathbf{B}_b dA + \int_A \mathbf{B}_s^T \bar{\mathbf{D}}_s \mathbf{B}_s dA \right), \bar{\mathbf{K}} = \mathbf{U}^{0T} \bar{\mathbf{K}} \mathbf{U}^0, \tag{45}$$

$$\mathbf{K}_G = \int_A \mathbf{B}_G^T \begin{bmatrix} 1 & 0 \\ 0 & k_1 \end{bmatrix} \mathbf{B}_G dA, K_G = \mathbf{U}^{0T} \mathbf{K}_G \mathbf{U}^0, \tag{46}$$

$$\mathbf{K}_m = \int_A \mathbf{N}^T \mathbf{D}_m \mathbf{N} dA, K_m = \mathbf{U}^{0T} \mathbf{K}_m \mathbf{U}^0, \tag{47}$$

$$B = \frac{\omega_0}{\lambda} \left( \frac{R}{(\bar{K}_{s=\lambda} - \alpha_1 N_{cr} K_G - \omega_0^2 K_m)} - \frac{R}{\bar{K}_{s=0} - \alpha_1 N_{cr} K_G - \omega_0^2 K_m} \right), \bar{K}_{s=\lambda} = \mathbf{U}^{0T} \left( \int_A \mathbf{B}^T \bar{\mathbf{D}}(s = \lambda) \mathbf{B} dA \right) \mathbf{U}^0. \tag{56}$$

$$\mathbf{R} = \int_A q \mathbf{N}_w dA, R = \mathbf{R} \mathbf{U}^0, \tag{48}$$

in which:

$$\mathbf{B}_b^i = \begin{bmatrix} 0 & -\mathbf{N}_{,x}^i & 0 \\ 0 & 0 & -\mathbf{N}_{,y}^i \\ 0 & -\mathbf{N}_{,y}^i & -\mathbf{N}_{,x}^i \end{bmatrix}, \mathbf{B}_s^i = \begin{bmatrix} \mathbf{N}_{,x}^i & -\mathbf{N}^i & 0 \\ \mathbf{N}_{,y}^i & 0 & -\mathbf{N}^i \end{bmatrix}, \mathbf{B}_G^i = \begin{bmatrix} \mathbf{N}_{,x}^i & 0 & 0 \\ \mathbf{N}_{,y}^i & 0 & 0 \end{bmatrix}, \tag{49}$$

$$\bar{\mathbf{D}}_b = h^3/12 \begin{bmatrix} 3K\bar{\eta} \frac{(2+\bar{\eta})}{(1+2\bar{\eta})} & 3K\bar{\eta} \frac{(1-\bar{\eta})}{(1+2\bar{\eta})} & 0 \\ 3K\bar{\eta} \frac{(1-\bar{\eta})}{(1+2\bar{\eta})} & 3K\bar{\eta} \frac{(2+\bar{\eta})}{(1+2\bar{\eta})} & 0 \\ 0 & 0 & 3/2K\bar{\eta} \end{bmatrix}, \tag{50}$$

$$\bar{\mathbf{D}}_s = hk \begin{bmatrix} 3/2K\bar{\eta} & 0 \\ 0 & 3/2K\bar{\eta} \end{bmatrix}, \bar{\eta} = s \int_0^\infty \eta(t) e^{-st} dt = c_1 + \frac{c_2 s}{s + \lambda}. \tag{51}$$

Equation (44) can be rewritten as follows:

$$(A\omega_0 + Bs) (\bar{K} - \alpha_1 N_{cr} K_G - \omega_0^2 K_m) = \omega_0 R. \tag{52}$$

Satisfying Eq. (52) at  $s = 0$ , Eq. (53) is obtained:

$$A\omega_0 (\bar{K}_{s=0} - \alpha_1 N_{cr} K_G - \omega_0^2 K_m) = \omega_0 R. \tag{53}$$

Consequently, the coefficients of the time function are determined as follows:

$$A = \frac{R}{\bar{K}_{s=0} - \alpha_1 N_{cr} K_G - \omega_0^2 K_m}, \bar{K}_{s=0} = \mathbf{U}^{0T} \left( \int_A \mathbf{B}^T \bar{\mathbf{D}}(s = 0) \mathbf{B} dA \right) \mathbf{U}^0, \tag{54}$$

$$B = \frac{\omega_0 \left( \frac{R}{(\bar{K} - \alpha_1 N_{cr} K_G - \omega_0^2 K_m)} - A \right)}{s}, \forall s > 0. \tag{55}$$

It is noted that for calculating  $B$ , although Eq. (55) is satisfied for every  $s > 0$ , our experience with the numerical solution of Eq. (87), which is related to the Bernoulli viscoelastic beam (Please study the Appendix 1), showed that the best value for  $s$  is  $s \approx \lambda$ . Thus, Eq. (56) is obtained:

Finally, the steady-state response of a Mindlin viscoelastic plate can be expressed as follows:

$$u(x,y,t) = u^0 \left( \frac{R}{\bar{K}_{s=0} - \alpha_1 N_{cr} K_G - \omega_0^2 K_m} \sin \omega_0 t + \frac{\omega_0}{\lambda} \left( \frac{R}{\bar{K}_{s=\lambda} - \alpha_1 N_{cr} K_G - \omega_0^2 K_m} - \frac{R}{\bar{K}_{s=0} - \alpha_1 N_{cr} K_G - \omega_0^2 K_m} \right) \cos \omega_0 t \right), \tag{57}$$

where  $\mathbf{u}^0 = \mathbf{u}(x,y,t = 0)$  is easily calculated utilizing the elastic bending analysis at time zero.

### Transient Response

The transient response of a Mindlin viscoelastic plate can be expressed as follows [24]:

$$u(x,y,t) = u^0 J(t), J(t) = e^{-\alpha_0 t} (C \sin \omega_0 t + D \cos \omega_0 t), \tag{58}$$

where  $\alpha_0$  is the viscous damping frequency.  $\alpha_0$  and  $\omega_0$  are calculated by solving Eq. (59) as follows:

$$\det(s_0 K^* + s_0^2 K_m - N_{cr} \alpha_1 K_G) = 0, s_0 = i\omega_0 - \alpha_0, \omega_0 \cong \Omega \sqrt{1 - \alpha_1}. \tag{59}$$

### Total Dynamic Response

Thus, the total dynamic response can be written as:

$$u(x,y,t) = u^0 (F(t) + J(t)) = u^0 [A \sin \omega_0 t + B \cos \omega_0 t + e^{-\alpha_0 t} (C \sin \omega_0 t + D \cos \omega_0 t)]. \tag{60}$$

**Table 1** The coefficients of the time function of simply supported Mindlin viscoelastic square plates with different materials ( $t_s = 1s, \alpha_1 = 0, H(t) = (1 - e^{-\alpha_0 t})(Asin\omega_0 t + Bcos\omega_0 t)$ )

	$\omega_0$		$\alpha_0$		A	B
	Present	[24]	Present	[24]		
$c_1 = 0.1$	18.18	18.18	0.29	0.29	-1.24	-35.79
$c_1 = 0.3$	18.18	18.18	0.22	0.22	-1.83	-45.04
$c_1 = 0.5$	18.18	18.18	0.16	0.16	-2.82	-63.56
$c_1 = 0.7$	18.18	-	0.1	-	-5.13	-112.38
$c_1 = 0.9$	18.19	-	0.03	-	-17.86	-467.12
$c_1 = 0.9.5$	18.19	-	0.016	-	-43.28	-1912.6

C and D can be calculated using the initial conditions at time zero:

$$w(x,y, t = 0) = 0 \Rightarrow D = -B, \tag{61}$$

$$\dot{w}(x,y, t = 0) = 0 \Rightarrow C = -B \frac{\alpha_0}{\omega_0} - A \cong -A, \frac{\alpha_0}{\omega_0} \ll 1. \tag{62}$$

In other words, the transient response can be rewritten as:

$$\mathbf{u}(x,y,t) = -\mathbf{u}^0 e^{-\alpha_0 t} (Asin\omega_0 t + Bcos\omega_0 t). \tag{63}$$

Finally, the total nonlinear dynamic response of Mindlin viscoelastic plates subjected to harmonic transversal load  $q(t) = q\sin\omega_0 t$  and in-plane compression  $N_x = \alpha_1 N_{cr}$  can be expressed as:

$$\mathbf{u}(x,y,t) = \mathbf{u}^0 H(t), H(t) = (1 - e^{-\alpha_0 t})(Asin\omega_0 t + Bcos\omega_0 t). \tag{64}$$

Equation (64) indicates that, due to the damping property of viscoelastic materials, the transient response is damped and the total response converges to the steady-state response.

### Numerical Results

In this section, the forced vibration analysis of viscoelastic plates subjected to harmonic transversal load and in-plane compression with different material properties are considered. The unknown coefficients of the total response, A, B,  $\omega_0$  and  $\alpha_0$ , are determined using Matlab programming. The geometrical and material properties are taken as  $h/a = 0.1, K = 3 \times 10^7 N/m^2, k = 5/6, \rho = 7800 Kg/m^2, c_1 + c_2 = 1$  and  $q = 10^5 N/m^2$ . Also, for spatial discretization, distribution of 25 nodes on the domain of the square plate is considered.

For calculating B, our experience with the numerical solution of Eq. (87), which is related to the Bernoulli viscoelastic beam, showed that the best value for s is  $s \approx \lambda$ . Therefore, in the range  $s \approx \lambda$ , several values are selected and the average of the obtained values for B is calculated.

**Table 2** The coefficients of the time function of simply supported Mindlin viscoelastic square plates with different materials ( $t_s = 1s, \alpha_1 = 0.5, H(t) = (1 - e^{-\alpha_0 t})(Asin\omega_0 t + Bcos\omega_0 t)$ )

	$\omega_0$	$\alpha_0$	A	B
$c_1 = 0.1$	12.9	0.56	-1.25	-26.07
$c_1 = 0.3$	12.9	0.438	-1.85	-33.14
$c_1 = 0.5$	12.9	0.31	-2.87	-47.63
$c_1 = 0.7$	12.9	0.18	-5.29	-88.08
$c_1 = 0.9$	12.9	0.06	-20.35	-546.05

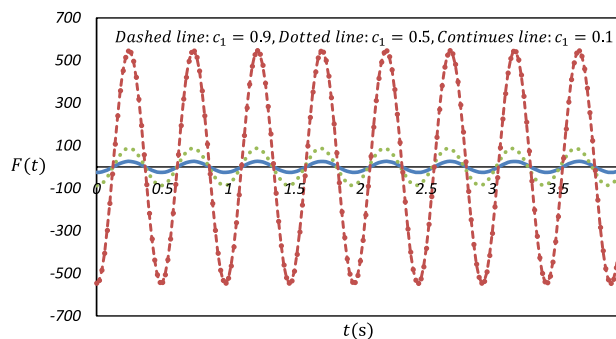


**Fig. 2** Steady-state responses of simply supported moderately thick viscoelastic square plates ( $h/L = 0.1, \alpha_1 = 0.5$ )

**Table 3** The coefficients of the time function of simply supported Mindlin viscoelastic square plates with different relaxation times ( $c_1 = 0.1, \alpha_1 = 0.5, \omega_0 = 12.9$ )

	A	B	$B/(\omega_0/\lambda)$
$t_s = 1s$	-1.24	-26.07	-2.02
$t_s = 10s$	-1.24	-260.7	-2.02
$t_s = 100s$	-1.24	-2670	-2.02

### Verification

Table 1 considers the effect of relaxation function parameter,  $c_1$ , on the time responses of moderately thick viscoelastic plates.

**Table 4** The coefficients of the time function of simply supported Mindlin viscoelastic square plates with different bulk moduli ( $c_1 = 0.1, \alpha_1 = 0.5, t_s = 1s$ )

	A	B	$\omega_0$	$B/(\omega_0/\lambda)$
$K = 3 \times 10^6$	-1.24	-8.26	4.09	-2.02
$K = 3 \times 10^7$	-1.24	-26.07	12.9	-2.02
$K = 3 \times 10^8$	-1.24	-82.6	40.9	-2.02

**Table 5** The coefficients of the time function of simply supported Mindlin viscoelastic square plates with different mass densities ( $c_1 = 0.1, \alpha_1 = 0.5, t_s = 1s$ )

	A	B	$\omega_0$	$B/(\omega_0/\lambda)$
$\rho = 5000$	-1.24	-32.56	16.12	-2.02
$\rho = 7800$	-1.24	-26.07	12.9	-2.02
$\rho = 10000$	-1.24	-22.93	11.4	-2.01
$\rho = 20000$	-1.24	-16.25	8.06	-2.01

**Table 6** The coefficients of the time function of simply supported Mindlin viscoelastic square plates subjected to different in-plane compressions ( $c_1 = 0.1, t_s = 1s$ )

	A	B	$\omega_0$	$B/(\omega_0/\lambda)$
$\alpha_1 = 0$	-1.24	-35.79	18.18	-2.02
$\alpha_1 = 0.1$	-1.24	-34.2	17.25	-1.98
$\alpha_1 = 0.3$	-1.24	-30.39	15.22	-1.99
$\alpha_1 = 0.5$	-1.25	-26.07	12.9	-2.02
$\alpha_1 = 0.7$	-1.25	-20.39	10.07	-2.02

As the results show, by increasing  $c_1$  which means the material tends to elasticity, the absolute value of the coefficients  $A$  and  $B$  are increased and the responses tend to the resonance behavior. So that, the maximum value of the time function corresponding to  $c_1 = 0.95$  is approximately 55 times of the maximum value of the time function related to  $c_1 = 0.1$ .

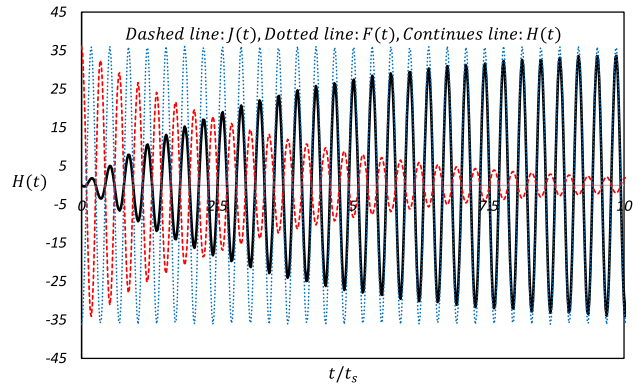
**Effect of Material Properties**

Table 2 investigates the effect of relaxation function parameter,  $c_1$ , on the time responses of moderately thick viscoelastic plates.

Figure 2 shows the steady-state responses of Mindlin viscoelastic square plates with simply supported boundary conditions subjected to harmonic transversal loading and in-plane compression.

**Table 7** The coefficients of the time function of a simply supported Mindlin viscoelastic square plate subjected to different transversal loadings ( $c_1 = 0.1, \alpha_1 = 0.5, t_s = 1s$ )

	A	B	$\omega_0$	$B/(\omega_0/\lambda)$
$q = 10^4$	-1.24	-26.07	12.9	-2.02
$q = 10^5$	-1.24	-26.07	12.9	-2.02
$q = 10^6$	-1.24	-26.07	12.9	-2.02



**Fig. 3** Transient  $J(t)$ , steady-state  $F(t)$ , and total dynamic  $H(t)$  responses of a simply supported moderately thick viscoelastic square plate under harmonic transversal loading ( $h/L = 0.1, c_1 = 0.1, \alpha_1 = 0, \alpha_0 = 0.29, \omega_0 = 18.18$ )

The results show that, by increasing  $c_1$ , the absolute value of the coefficients  $A$  and  $B$  are increased and the responses tend to the resonance behavior.

Table 3 investigates the effect of relaxation time,  $t_s$ , on the time responses of moderately thick viscoelastic plates.

The results show that the absolute value of  $B$  is linearly related to the relaxation time, so that  $B/(\omega_0/\lambda)$  does not change by changing the relaxation time. Also,  $A$  does not change by changing the relaxation time.

Tables 4–5 consider the effect of bulk modulus and mass density on the time responses of moderately thick viscoelastic plates.

As the results illustrate  $B/(\omega_0/\lambda)$  and  $A$  do not change by changing the bulk modulus.

As the results show, the absolute value of  $B$  is decreased by increasing mass density. But  $B/(\omega_0/\lambda)$  and  $A$  do not change by changing the mass density.

**Effect of Loading**

Tables 6, 7 consider the effect of in-plane compression and transversal loading on the time responses of moderately thick viscoelastic plates.



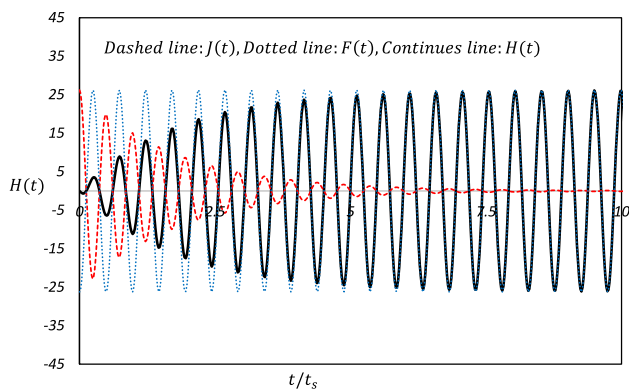


**Fig. 4** Transient  $J(t)$ , steady-state  $F(t)$ , and total dynamic  $H(t)$  responses of a simply supported moderately thick viscoelastic square plate under harmonic transversal loading and in-plane compression ( $h/L = 0.1, c_1 = 0.1, \alpha_1 = 0.5, \alpha_0 = 0.57, \omega_0 = 12.9$ )

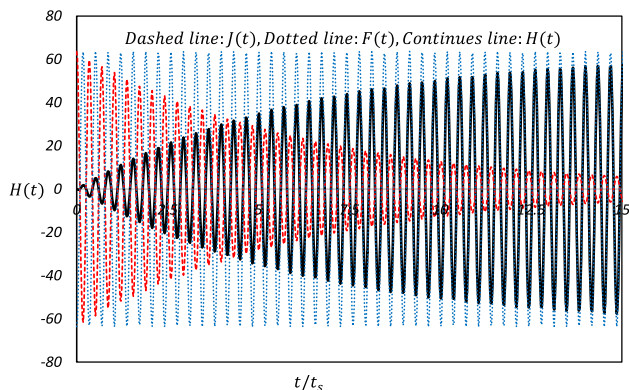


**Fig. 5** Transient  $J(t)$ , steady-state  $F(t)$ , and total dynamic  $H(t)$  responses of a simply supported moderately thick viscoelastic square plate under harmonic transversal loading ( $h/L = 0.1, c_1 = 0.5, \alpha_1 = 0, \alpha_0 = 0.16, \omega_0 = 18.18$ )

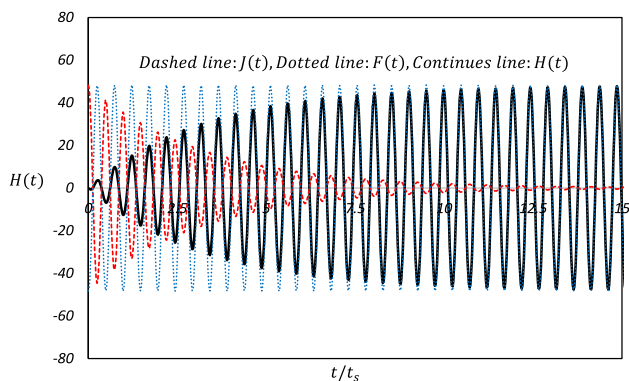


**Fig. 6** Transient  $J(t)$ , steady-state  $F(t)$ , and total dynamic  $H(t)$  responses of a simply supported moderately thick viscoelastic square plate under harmonic transversal loading and in-plane compression ( $h/L = 0.1, c_1 = 0.5, \alpha_1 = 0.5, \alpha_0 = 0.31, \omega_0 = 12.9$ )

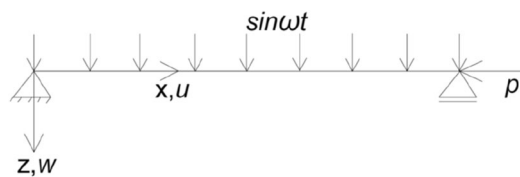


**Fig. 7** A simply supported viscoelastic beam subjected to harmonic transversal load and axial compression

As the results illustrate, by increasing the in-plane compression, the absolute value of  $B$  is decreased. But  $B/(\omega_0/\lambda)$  and  $A$  are almost constant.

The results show that  $A$  and  $B$  do not change by changing the value of the distributed load.

### Total Dynamic Responses

Employing Eq. (64), Figs. 3, 4, 5, 6 show the transient, steady-state and total dynamic responses of Mindlin viscoelastic square plates with simply supported boundary conditions subjected to harmonic transversal loading and in-plane compression.

The results indicate that, due to the damping property of viscoelastic materials, the transient responses are damped and the total responses converge to the steady-state responses.

### Conclusions

In this research, a novel formulation was introduced while the transient, steady-state and total dynamic responses of Mindlin viscoelastic plates under out-of-plane and in-plane loadings are explicitly formulated in the time domain for the first time.

The results show that the total dynamic responses of Mindlin viscoelastic plates subjected to harmonic transversal load  $q(t) = q\sin\omega_0t$ , the excitation frequency is considered as equal to the natural frequency, and in-plane compression  $N_x = \alpha_1 N_{cr}$  can be expressed as  $u = u^0(1 - e^{-\alpha_0 t})(A\sin\omega_0 t + B\cos\omega_0 t)$  in which  $A = \frac{R}{K_{\omega=0} - \alpha_1 N_{cr} K_G - \omega_0^2 K_m}$ , and  $B = \frac{\omega_0}{\lambda} \left( \frac{R}{K_{\omega=\lambda} - \alpha_1 N_{cr} K_G - \omega_0^2 K_m} - A \right)$  and  $u^0$  is calculated using the elastic bending analysis at time zero.

Also, the results indicate that the absolute value of  $B$  is linearly related to the relaxation time. Besides,  $A$  and  $B/(\omega_0/\lambda)$  do not change by changing the relaxation time, bulk modulus, density, and transversal load.

The results show that by increasing  $c_1$  which means the material tends to elasticity, the responses tend to the resonance behavior.

## Appendix 1

### Forced Vibration Analysis of Simply Supported Bernoulli Viscoelastic Beams Subjected to Harmonic Transversal Load and Axial Compression

The equation of a Bernoulli viscoelastic beam subjected to a harmonic transversal load and axial compression, (as illustrated in Fig. 7) can be written as follows [28]:

$$\frac{\partial^2 M}{\partial x^2} - \rho \frac{\partial^2 w}{\partial t^2} = \rho \frac{\partial^2 w}{\partial t^2} - q(t), \quad (65)$$

in which  $M$  is the bending moment,  $w$  is the transversal deflection,  $t$  is the time and  $\rho$  is the mass per unit length.

The bending moment can be expressed as:

$$M = \int_A \sigma(x, t) z dA. \quad (66)$$

The stress–strain relation of a linear viscoelasticity based on the Boltzmann integral can be defined as [26]:

$$\sigma(x, t) = E(t)\varepsilon(0) + \int_0^t E(t - \tau)\dot{\varepsilon}(\tau)d\tau, \quad \dot{\varepsilon}(t) = \partial\varepsilon/\partial t, \quad (67)$$

where  $E(t)$  is the modulus of elasticity.

For Bernoulli beams, the strain–deflection relation can be written as:

$$\varepsilon(x, t) = -z \frac{\partial^2 w(x, t)}{\partial x^2}. \quad (68)$$

Investigating simply supported boundary conditions, the deflection may be approximated using the separation of variables method as follows:

$$w(x, t) = F(t) \sin \frac{\pi x}{l}. \quad (69)$$

It is noted that only one term of the series of  $\sin \frac{n\pi x}{l}$  has been considered, since the goal of this step is to concentrate on the time domain solution.

The time-dependent elasticity modulus can be expressed as:

$$E(t) = E_0 \eta(t), E_0 = E(t = 0), \quad (70)$$

in which  $\eta(t)$  is the relaxation function of viscoelastic material which is defined in Eq. (9).

Substituting Eqs. (66–70) into Eq. (65), Eq. (71) is obtained:

$$E_0 \eta(t) \frac{I\pi^4}{l^4} F(0) + E_0 \frac{I\pi^4}{l^4} \int_0^t \eta(t - \tau) \dot{F}(\tau) d\tau - \frac{\pi^2}{l^2} p F(t) + m \ddot{F}(t) = q(t), \quad (71)$$

where  $I = \int_A z^2 dA$  is the moment of inertia.

The compressive load may be given as:

$$p = \alpha_1 P_e, P_e = \frac{\pi^2 E_0 I}{l^2}, 0 \leq \alpha_1 < 1, \quad (72)$$

in which  $\alpha_1$  is constant.

For Bernoulli viscoelastic plates,  $\Omega$  is defined as the fundamental natural frequency calculated by the free vibration analysis of Bernoulli viscoelastic beams at time zero,  $\Omega^2 = \frac{E_0 I \pi^4}{m l^4}$ . If the beam is subjected to axial compression too, the natural frequency is decreased  $\omega_0 = \Omega \sqrt{1 - \alpha_1}$ , [24]. In this paper, the beam is subjected to harmonic transversal load  $q(t) = q_0 \sin \omega_0 t$  and axial compression, simultaneously. In other word, the excitation frequency is equal to the natural frequency and the time-dependent behavior of the viscoelastic beam is studied.

Replacing Eq. (72) in Eq. (71), Eq. (73) is obtained:

$$\eta(t) F(0) + \int_0^t \eta(t - \tau) \dot{F}(\tau) d\tau - \alpha_1 F(t) + \frac{\ddot{F}(t)}{\Omega^2} = q_0 \sin \omega_0 t, \quad (73)$$

$$\Omega^2 = \frac{E_0 I \pi^4}{m l^4}, q_0 = \frac{q l^4}{\pi^4 E_0 I}.$$

Equation (73) can be simplified as follows:

$$s F^* \eta^* - \alpha_1 F^* + \frac{\ddot{F}^*}{\Omega^2} = q_0 (\sin \omega_0 t)^*, \eta^* = \frac{c_1}{s} + \frac{c_2}{s + \lambda}, \quad (74)$$

in which  $\eta^*$ ,  $F^*$ ,  $\ddot{F}^*$  and  $(\sin \omega_0 t)^*$  are the Laplace transformation of  $\eta(t)$ ,  $F(t)$ ,  $\ddot{F}(t)$  and  $\sin \omega_0 t$ , respectively.

For the steady-state response, the time function is approximated as follows:

$$F(t) = A \sin \omega_0 t + B \cos \omega_0 t. \quad (75)$$

Hence, Eqs. (76–77) are derived:

$$\ddot{F}(t) = -A \omega_0^2 \sin \omega_0 t - B \omega_0^2 \cos \omega_0 t = -\omega_0^2 F(t), \quad (76)$$

$$\ddot{F}^* = -\omega_0^2 F^*. \quad (77)$$

Inserting Eq. (77) into Eq. (74), Eq. (78) is obtained:

$$sF^* \eta^* - \alpha_1 F^* - \frac{\omega_0^2 F^*}{\Omega^2} = q_0 (\sin \omega_0 t)^*, \omega_0^2 = \Omega^2 (1 - \alpha_1). \tag{78}$$

Equation (78) can be simplified as follows:

$$F^* (\bar{\eta} - 1) = q_0 (\sin \omega_0 t)^*, \bar{\eta} = s \eta^*. \tag{79}$$

On the other hand:

$$F^* = \frac{A\omega_0 + Bs}{s^2 + \omega_0^2}, (\sin \omega_0 t)^* = \frac{\omega_0}{s^2 + \omega_0^2}. \tag{80}$$

Supposing  $c_1 + c_2 = 1$  and by substituting Eqs. (80) into Eq. (79), Eq. (81) is derived:

$$(A\omega_0 + Bs) \left( -\frac{c_2 \lambda}{s + \lambda} \right) = q_0 \omega_0 \tag{81}$$

or

$$-c_2 \lambda (A\omega_0 + Bs) = q_0 \omega_0 (s + \lambda). \tag{82}$$

If Eq. (82) is solved by unifying the sentences:

$$A = -\frac{q_0}{c_2}, \tag{83}$$

$$B = -\frac{q_0 \omega_0}{c_2 \lambda}. \tag{84}$$

Therefore, the steady-state response of a Bernoulli viscoelastic beam can be expressed as follows

$$w(x, t) = -\frac{q_0}{c_2} \left( \sin \omega_0 t + \frac{\omega_0}{\lambda} \cos \omega_0 t \right) \sin \frac{\pi x}{l}. \tag{85}$$

But, if Eq. (82) is solved numerically:

$$s = 0 \Rightarrow A = -\frac{q_0}{c_2}, \tag{86}$$

$$B = \omega_0 \left( \frac{q_0 (s + \lambda)}{-c_2 \lambda} - A \right) / s, \forall s > 0. \tag{87}$$

Although Eq. (87) is hold  $\forall s > 0$ , the numerical solution showed that selecting the large value for  $s$ , decreases the accuracy. And selecting  $s \approx \lambda$  is the proper selection.

On the other hand, the transient response of a Bernoulli viscoelastic beam can be expressed as follows [24]:

$$w(x, t) = \sin \frac{\pi x}{l} J(t), J(t) = e^{-\alpha_0 t} (C \sin \omega_0 t + D \cos \omega_0 t),$$

$$\omega_0 = \Omega \sqrt{1 - \alpha_1}, \alpha_0 = \frac{c_2 \lambda}{2(1 - \alpha_1)}. \tag{88}$$

Thus, the total dynamic response can be written as:

$$w(x, t) = \sin \frac{\pi x}{l} (F(t) + J(t)) = w(x, t = 0) \left[ -\frac{q_0}{c_2} \sin \omega_0 t - \frac{q_0 \omega_0}{c_2 \lambda} \cos \omega_0 t + e^{-\alpha_0 t} (C \sin \omega_0 t + D \cos \omega_0 t) \right]. \tag{89}$$

$C$  and  $D$  can be calculated using the initial conditions at time zero:

$$w(x, t = 0) = 0 \Rightarrow D = \frac{q_0 \omega_0}{c_2 \lambda}, \tag{90}$$

$$\dot{w}(x, t = 0) = 0 \Rightarrow C = -B \frac{\alpha_0}{\omega_0} - A \cong \frac{q_0}{c_2}, \frac{\alpha_0}{\omega_0} \ll 1. \tag{91}$$

In other words, the transient response can be written as:

$$w(x, t) = w(x, t = 0) e^{-\alpha_0 t} \left( \frac{q_0}{c_2} \sin \omega_0 t + \frac{q_0 \omega_0}{c_2 \lambda} \cos \omega_0 t \right). \tag{92}$$

Finally, the total dynamic response of Bernoulli viscoelastic plates subjected to harmonic transversal load  $q(t) = q \sin \omega_0 t$  and axial compression  $p = \alpha_1 P_e$  can be expressed as:

$$w(x, t) = w(x, t = 0) H(t), H(t) = (1 - e^{-\alpha_0 t}) \left( -\frac{q_0}{c_2} \sin \omega_0 t - \frac{q_0 \omega_0}{c_2 \lambda} \cos \omega_0 t \right). \tag{93}$$

## Appendix 2

### Constructing the Simple hp Cloud Approximation Functions

Considering a selected set of scattered nodes as illustrated in Fig. 8:

$$\mathbf{Q}_N = \{ \mathbf{x}_1, \mathbf{x}_2, \dots, \mathbf{x}_N \}. \tag{94}$$

Each node is centered at  $\mathbf{x}_i$ , related to the elliptical cloud  $\varphi_i$  and has the effective radius  $h_{ix}$  and  $h_{iy}$ .

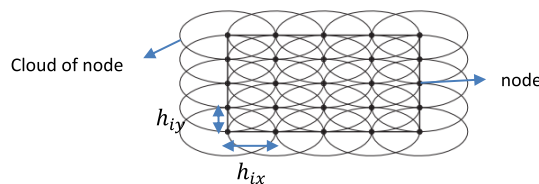


Fig. 8 Distribution of 25 nodes on the domain of a rectangular plate

The basis functions, the simple hp cloud meshless approximation functions, are defined as:

$$\mathbf{N}^i(\mathbf{x}) = \psi_i(\mathbf{x})\mathbf{L}_i(\mathbf{x}), \quad (95)$$

where  $\psi_i$  are the Shepard functions and  $\mathbf{L}_i$  are the complete polynomial of order 2 as follows:

$$\mathbf{L}_i = [1x - x_i y - y_i(x - x_i)^2(x - x_i)(y - y_i)(y - y_i)^2]. \quad (96)$$

By defining the weight functions as:

$$\begin{aligned} W_i(\mathbf{x}) &= 1 - 6r_i^2 + 8r_i^3 + 3r_i^4, r_i(\mathbf{x}) \\ &= \sqrt[2]{\left(\frac{x - x_i}{h_{ix}}\right)^2 + \left(\frac{y - y_i}{h_{iy}}\right)^2}, r_i \leq 1. \end{aligned} \quad (97)$$

Shepard functions are calculated in the following form:

$$\psi_i(\mathbf{x}) = \frac{W_i(\mathbf{x})}{\sum_{\beta} W_{\beta}(\mathbf{x})}. \quad (98)$$

## Declarations

**Conflict of interest** The authors declare that they have no conflict of interest.

## References

- Wang Y, Tsai T (1988) Static and dynamic analysis of a viscoelastic plate by the finite element method. *Appl Acoust* 25:77–94. [https://doi.org/10.1016/0003-682X\(88\)90017-5](https://doi.org/10.1016/0003-682X(88)90017-5)
- Ilyasov MH, Akoz AY (2000) The vibration and dynamic stability of viscoelastic plates. *Int J Eng Sci* 38:695–714. [https://doi.org/10.1016/S0020-7225\(99\)00060-9](https://doi.org/10.1016/S0020-7225(99)00060-9)
- Eshmatov BK (2007) Nonlinear vibrations and dynamic stability of viscoelastic orthotropic rectangular plates. *J Sound Vib* 300:709–726. <https://doi.org/10.1016/j.jsv.2006.08.024>
- Abdoun F, Azrar L, Potier-Ferry M (2009) Forced harmonic response of viscoelastic structures by an asymptotic. *Comput Struct* 87:91–100. <https://doi.org/10.1016/j.compstruc.2008.08.006>
- Gupta AK, Khanna A, Kumar S, Kumar M, Gupta DV, Sharma P (2010) Vibration analysis of visco-elastic rectangular plate with thickness varies linearly in one and parabolically in other direction. *Adv Stud Theor Phys* 4(13):743–758. <https://doi.org/10.4236/am.2010.12017>
- Li JJ, Cheng CJ (2010) Differential quadrature method for analyzing nonlinear dynamic characteristics of viscoelastic plates with shear effects. *Nonlinear Dyn* 61:57–70. <https://doi.org/10.1007/s11071-009-9631-8>
- Shariyat M (2011) A double-superposition global–local theory for vibration and dynamic buckling analyses of viscoelastic composite/sandwich plates: a complex modulus approach. *Arch Appl Mech* 81:1253–1268. <https://doi.org/10.1007/s00419-010-0483-y>
- Mahmoudkhani S, Haddadpour H, Navazi HM (2012) Free and forced random vibration analysis of sandwich plates with thick viscoelastic cores. *J Vib Control* 19(14):2223–2240. <https://doi.org/10.1177/1077546312456229>
- Temel B, Sahan MF (2013) Transient analysis of orthotropic, viscoelastic thick plates in the Laplace domain. *Eur J Mech A-Solids* 37:96–105. <https://doi.org/10.1016/j.euromechsol.2012.05.008>
- Amabili M (2016) Nonlinear vibration of viscoelastic rectangular plates. *J Sound Vib* 362:142–156. <https://doi.org/10.1016/j.jsv.2015.09.035>
- Wan H, Li Y, Zheng L (2016) Vibration and damping analysis of a multilayered composite plate with a viscoelastic midlayer. *Shock Vib*. <https://doi.org/10.1155/2016/6354915>
- Khadem Moshir S, Eipakchi H, Sohani F (2017) Free vibration behavior of viscoelastic annular plates using first order shear deformation theory. *Struct Eng Mech* 62(5):607–618. <https://doi.org/10.12989/sem.2017.62.5.607>
- Amabili M (2018) Nonlinear damping in nonlinear vibrations of rectangular plates: derivation from viscoelasticity and experimental validation. *J Mech Phys Solids* 118:275–292. <https://doi.org/10.1016/j.jmps.2018.06.004>
- Balasubramanian P, Ferrari G, Amabili M (2018) Identification of the viscoelastic response and nonlinear damping of a rubber plate in nonlinear vibration regime. *Mech Syst Signal Process* 111:376–398. <https://doi.org/10.1016/j.ymsp.2018.03.061>
- Zhou YF, Wang ZM (2019) Dynamic instability of axially moving viscoelastic plate. *Eur J Mech A-Solids* 73:1–10. <https://doi.org/10.1016/j.euromechsol.2018.06.009>
- Rouzegar J, Davoudi M (2020) Forced vibration of smart laminated viscoelastic plates by RPT finite element approach. *Acta Mech Sin* 36(4):933–949. <https://doi.org/10.1007/s10409-020-00964-1>
- Silva VA, De Lima AMG, Ribeiro LP, Da Silva AR (2020) Uncertainty propagation and numerical evaluation of viscoelastic sandwich plates having nonlinear behavior. *J Vib Control* 26:447–458. <https://doi.org/10.1177/1077546319889816>
- Sofiyev AH, Zerir Z, Kuruoglu N (2020) Dynamic behavior of FGM viscoelastic plates resting on elastic foundations. *Acta Mech* 231:1–17. <https://doi.org/10.1007/s00707-019-02502-y>
- Ojha RK, Dwivedy SK (2020) Dynamic analysis of a three-layered sandwich plate with composite layers and leptaenia pyrotechnica rheological elastomer-based viscoelastic core. *J Vib Eng Technol* 8:541–553. <https://doi.org/10.1007/s42417-019-00129-w>
- Amabili M, Balasubramanian P, Ferrari G (2020) Nonlinear vibrations and damping of fractional viscoelastic rectangular plates. *Nonlinear Dyn* 103:3581–3609. <https://doi.org/10.1007/s11071-020-05892-0>
- Zamani HA (2020) Free vibration of viscoelastic foam plates based on single-term Bubnov-Galerkin, least squares, and point collocation methods. *Mech Time-Depend Mater* 25:495–512. <https://doi.org/10.1007/s11043-020-09456-y>
- Jafari N, Azhari M (2021) Free vibration analysis of viscoelastic plates with simultaneous calculation of natural frequency and viscous damping. *Math Comput Simul* 185:646–659. <https://doi.org/10.1016/j.matcom.2021.01.019>
- Jafari N (2022) Non-Harmonic resonance of viscoelastic structures subjected to time-dependent decreasing exponential transversal distributed loads. *Earthq Eng Vib*, in Press.
- Jafari N, Azhari M (2022) Dynamic stability analysis of Mindlin viscoelastic plates subjected to constant and harmonic in-plane compressions based on free vibration analysis of elastic plates. *Acta Mech*. <https://doi.org/10.1007/s00707-022-03215-5>

25. Amabili M (2018) *Nonlinear Mechanics of Shells and Plates: Composite, Soft and Biological Materials*. Cambridge University Press, Cambridge
26. Zhang NH, Cheng CJ (1998) Nonlinear mathematical model of viscoelastic thin plates with its applications. *Comput Methods Appl Mech Eng* 16(5):307–319. [https://doi.org/10.1016/S0045-7825\(98\)00039-5](https://doi.org/10.1016/S0045-7825(98)00039-5)
27. Jafari N, Azhari M (2017) Stability analysis of arbitrarily shaped moderately thick viscoelastic plates using Laplace-Carson transformation and a simple hp cloud method. *Mech Time-Depend Mater* 21(3):365–381. <https://doi.org/10.1007/s11043-016-9334-8>
28. Szyszkowski W, Glockner PG (1985) The stability of viscoelastic perfect column: a dynamic approach. *Int J Solids Struct* 21(6):545–559. [https://doi.org/10.1016/0020-7683\(85\)90014-9](https://doi.org/10.1016/0020-7683(85)90014-9)

**Publisher's Note** Springer Nature remains neutral with regard to jurisdictional claims in published maps and institutional affiliations.

Springer Nature or its licensor holds exclusive rights to this article under a publishing agreement with the author(s) or other rightsholder(s); author self-archiving of the accepted manuscript version of this article is solely governed by the terms of such publishing agreement and applicable law.